

# Explicit versus Implicit Solvent Modeling of Raman Optical Activity Spectra

Kathrin H. Hopmann,<sup>\*,†</sup> Kenneth Ruud,<sup>†</sup> Magdalena Pecul,<sup>†,‡</sup> Andrzej Kudelski,<sup>‡</sup> Martin Dračinský,<sup>§</sup> and Petr Bour<sup>\*,§</sup>

<sup>†</sup>Centre for Theoretical and Computational Chemistry (CTCC), Department of Chemistry, University of Tromsø, N-9037 Tromsø, Norway

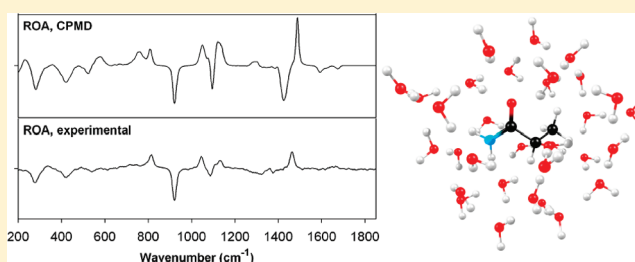
<sup>‡</sup>Department of Chemistry, Warsaw University, Pasteura 1, 02-093 Warsaw, Poland

<sup>§</sup>Institute of Organic Chemistry and Biochemistry, Academy of Sciences, Flemingovo nám. 2, 166 10 Prague, Czech Republic

**S** Supporting Information

**ABSTRACT:** Raman and Raman optical activity (ROA) spectra of molecules reflect not only molecular structure and conformation but also the dynamics and interactions with the solvent. For polar, biologically relevant molecules in aqueous environment, this often complicates the band assignment and interpretation of the spectra. In the present study, implicit dielectric and explicit solvent models are compared with respect to the influence of the choice of solvent model on the spectral shape. Lactamide and 2-aminopropanol were selected as model compounds, and the Raman and ROA spectra were measured for both enantiomers.

Geometries of explicitly solvated clusters were derived from quantum-mechanical calculations, classical (MD), and Car–Parrinello (CPMD) molecular dynamics. The results indicate that although the dielectric model reasonably well reproduces the main spectral features, more faithful intensity profiles, including the inhomogeneous band broadening, are obtained from the explicit MD and CPMD clusters. Additionally, the CPMD clusters are capable of reproducing most spectral features better than the classical dynamics, provided the simulation time is long enough to allow for a complete sampling of the conformational space. The hydrogen-bonded water molecules of the first hydration shell significantly influence the spectral intensities, whereas the effect of loosely attached or distant solvent molecules is minor. In order to average the signal, however, a relatively large number of MD geometries need to be considered, as was also exemplified by simulations of the ROA spectrum of the achiral molecule glycine. An explicit solvent modeling of sizable systems thus requires extensive computations, which became possible only recently due to the development of efficient analytical computational techniques.



## INTRODUCTION

Raman optical activity (ROA) spectroscopy,<sup>1,2</sup> which measures the difference in scattering of left- and right-circularly polarized light in chiral systems, is able to provide unique information not only about absolute molecular configuration<sup>3</sup> but also about molecular dynamics and interactions with the environment.<sup>4</sup> ROA has been applied to peptides,<sup>5–7</sup> proteins,<sup>8,9</sup> nucleic acids,<sup>10</sup> and even viruses.<sup>11</sup> Recently, it has also been demonstrated that it is possible to combine the effect with surface enhancement on silver nanostructured surfaces.<sup>12,13</sup>

ROA is very sensitive to details in molecular structure, and interpretations of ROA spectra therefore usually rely on quantum-chemical simulations.<sup>3,14,15</sup> For example, when theoretical spectra of possible species can be simulated precisely, conformational ratios can be obtained from experimental ROA spectra, with an accuracy comparable to NMR.<sup>16</sup> In many cases, however, in particular for biologically relevant polar molecules in the aqueous environment, an incomplete account of the solvent effects causes large errors in simulated spectra and in the subsequent analysis of

the experiment.<sup>17,18</sup> For strong solvent–solute interactions, such as hydrogen bonding, simplified solvent models may not be adequate.<sup>19</sup> Additionally, for some low-frequency modes, it is difficult to separate the solvent and solute spectral signal.<sup>20</sup> It is therefore of importance to better understand the effect of solvent interactions on the spectra and to establish computational strategies comprising the most important solvent effects.

The inclusion of the environment has become a standard part of *ab initio* simulations, since it leads to a better understanding and description of molecular energetics, structure, interactions, and dynamics of experimentally investigated systems. The probably oldest implicit solvent model, the Onsager reaction field, considers the solvated molecules as contained within a spherical cavity in an infinite, polarizable dielectric medium.<sup>21,22</sup> More universal approaches preferred today model the molecular cavity

**Received:** November 8, 2010

**Revised:** February 28, 2011

**Published:** March 21, 2011

more realistically and allow other interactions than the dipolar solute–solvent effects to be taken into account. Various boundary conditions are imposed to obtain a self-consistent response to the polarization induced in the solvent. For example, the original version of the popular COSMO model<sup>23</sup> treated the solvent as a perfect conductor. Other polarizable continuum models (PCM) treat the solvent as a dielectric.<sup>24</sup> The integral formulation of PCM<sup>25</sup> allows the model to be extended to more general solvation models. Alternatively (or additionally to the PCM approach), individual solvent molecules can be directly included in the computations, an approach also pursued in the present study. The explicitly solvated geometries can be obtained *ad hoc*, from quantum-mechanical, or classical molecular dynamical simulations. These explicit approaches are usually more time-consuming than the implicit models and bring additional challenges with respect to conformational and positional averaging over differently hydrated structures.

The adequacy of the implicit or explicit solvent models depends on the molecular property that is modeled. For example, reasonable energies and structures can be obtained by means of standard PCM,<sup>26,27</sup> while vibrational frequencies can be improved only partially.<sup>28</sup> In particular, vibrational properties of polar groups making directional hydrogen bonds to the solute are better described by point-charge-like solvent approximations.<sup>19,29,30</sup> Improved reproduction of VCD spectra requires inclusion of hydrogen-bonding effects arising from interaction with solvent or other solute molecules.<sup>31,32</sup> Electronic spectra are more problematic since solvent orbitals may participate in the solute electronic transitions. Modeling of electronically excited states thus often requires that explicit solvent molecules are included as part of the quantum-mechanical system<sup>33</sup> or adaptations of PCMs.<sup>34,35</sup> Solvent effects on nuclear magnetic resonance shielding are particularly difficult to reproduce by means of PCM because of the valence repulsion (true quantum solute–solvent interactions) as well as the bulk magnetizability not included in contemporary continuum models.<sup>36–38</sup> For modeling of Raman<sup>39</sup> and ROA<sup>40</sup> spectra, PCM approaches have previously been applied with varying degree of success.<sup>41</sup> Inclusion of explicit water molecules to model the first hydration shell has been shown to have significant effects on Raman<sup>42</sup> and ROA<sup>17,32</sup> spectra leading to better reproduction of experimental results. An alternative approach for generation of hydrated clusters involves the use of dynamical methods, such as molecular dynamics or Monte Carlo simulations.<sup>43,44</sup> Such time-consuming approaches are possible only due to the recent developments of analytic derivative techniques for calculating ROA intensities.<sup>45–47</sup> To our knowledge, however, unlike for NMR spectra,<sup>48</sup> Car–Parrinello molecular dynamics<sup>49</sup> (CPMD) has not been used previously to generate solvent–solute clusters in ROA calculations.

In the present study we investigate the role of the aqueous environment on the Raman and ROA spectra of two conformationally flexible and strongly hydrated compounds (lactamide and 2-aminopropanol, see Figure 1). The chosen model compounds are small enough to allow for accurate computations, and

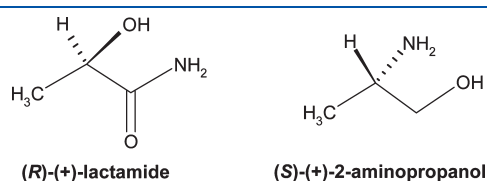


Figure 1. Chiral model molecules.

they contain typical functional groups mediating interactions in biomolecules. Different hydration models are analyzed, including polarizable continuum models, explicit *ad hoc* hydration, and two dynamical approaches, classical MD and CPMD. The detailed discussion focuses mostly on the lactamide molecule. The results for 2-aminopropanol are qualitatively similar, and the details are summarized in the Supporting Information. For the achiral molecule glycine, MD studies are performed to investigate artifacts caused by incomplete averaging. Equilibrium structures and the Raman and ROA spectra for the two chiral model compounds are discussed. The conformational space is first explored with quantum-chemical methods (vacuum and the conductor-like polarizable continuum model, CPCM) on the free molecule by performing scans of the potential energy surfaces. Equilibrium structures are then reoptimized in presence of some explicit water molecules (3–5). More extensively hydrated conformations are obtained from dynamical (MD and CPMD) methods and are compared to the QM results. The ROA and Raman spectra calculated by these approaches (CPCM, explicit waters, MD, CPMD) are analyzed and compared with experiment. The importance of the surrounding water shells, the number of necessary MD snapshots, and the advantages and drawbacks of using CPMD versus MD are discussed.

## METHODOLOGY

**Experimental Section.** The backscattering Raman and ROA spectra of lactamide and 2-aminopropanol (Figure 1) were measured for aqueous solutions, using the ChiralRAMAN instruments at the University of Warsaw and at the Academy of Sciences, Prague, manufactured by BioTools Inc., partially based on the design described by Werner Hug.<sup>50,51</sup> These instruments were equipped with frequency-doubled Nd:YVO<sub>4</sub> lasers providing radiation of 532 nm (Spectra-Physics Millennia Pro 2s). Further details of the optical design of the instrument can be found elsewhere.<sup>12,52</sup> All reagents were of high purity or analytical grade and were used as purchased from commercial companies, or additionally purified by active carbon, which provided a more stable signal in the lowest wavenumber region. The solutions were prepared with water of resistivity of ca. 18 MΩ · cm; the purification was carried out with a Millipore ultrapure water system. The accumulation time was 12 h, laser power at the laser head 360 mW (Prague) or 1.5 W (Warsaw), concentration 100 mg/mL, and cell volume 50 μL. The lactamide spectra collected at the Academy of Sciences, Prague, are presented, whereas for 2-aminopropanol we present the data from University of Warsaw. The water baseline was subtracted from the Raman spectra, and minor baseline corrections were done both for Raman and ROA.

**Single Molecule Geometry Optimization.** Free (*R*)-lactamide conformers were optimized using the B3LYP<sup>53,54</sup>/aug-cc-pVTZ<sup>55</sup> method as implemented in GAUSSIAN,<sup>56</sup> both in vacuum and by employing the CPCM<sup>23,26,27</sup> aqueous solvent correction. Systematic scans of the potential energy surface (PES) were performed, first with the O=C–C–H angle constrained (0 to 350° in 10° increments with the (O=C)–C–O–H angle initially set to either 0 or 180°, which provided a total of 72 starting conformations), followed by unconstrained optimization. For (*S*)-2-aminopropanol, a similar procedure was employed, but with the N–C–C–O angle fixed initially in 10° increments (and employing B3LYP/6-311++G(d,p)/CPCM). Frequency calculations at the same level of theory as the geometry optimizations were performed to confirm the nature of all stationary states. For

lactamide, the identified local minimum conformations were reoptimized at other levels of approximation (B3LYP/6-311++G(d,p)/CPCM, MP2/aug-cc-pVTZ/CPCM, and B3LYP/aug-cc-pVTZ/IEFPCM), which did not qualitatively change the results.

**Ad Hoc Hydration.** To explore basic changes caused by formation of the hydrogen bonds to the solvent, 3–5 water molecules were added to the optimized (*R*)-lactamide and (*S*)-2-aminopropanol conformers. The geometries of the hydrated clusters were optimized at the B3LYP/6-311++G(d,p)/CPCM level.

**MD Simulations.** Molecular dynamics calculations were performed within the TINKER software environment,<sup>57</sup> using the Amber99 force field.<sup>58</sup> Some torsion angle parameters involving the OH group were added manually, based on the serine Amber99 force field. For 2-aminopropanol, the charges for NH<sub>2</sub> were based on the OPLSAA force field.<sup>59</sup>

One solute ((*R*)-lactamide or (*S*)-2-aminopropanol) molecule was placed in a cubic water box (the length of a side being 18.56 Å), with 214 water molecules in total. Following initial minimization and equilibration (10 000 MD steps, 1 fs integration time), MD trajectories were run for 1–10 ns at constant temperature (298 K) and pressure (1 atm, NPT ensemble). Weighted histogram analysis (WHAM)<sup>60,61</sup> was also performed with a local version of the TINKER program for the lactamide  $\psi$  angle rotation, using 10 frames, each of 100 000 MD steps; control computation with 1 000 000 MD steps did not lead to significant changes on the resulting potential of mean force (PMF).

**CPMD Simulations.** Periodic boxes containing 30 water molecules and one solute molecule were created by the HYPERCHEM program.<sup>62</sup> The dimension of the box was 10.051 Å for lactamide and 10.066 Å for 2-aminopropanol. Using HYPERCHEM, an MD run was performed for 1 ns with 1 fs integration time steps and temperature 400 K to equilibrate the systems. The TIP3P<sup>63</sup> force field as part of Amber99 was used for water. As the next step, the geometry was optimized and transferred to the CPMD<sup>64</sup> software package. The same periodic boundary conditions and 4 au (0.09676 fs) time step were maintained for all CPMD calculations performed with the BLYP<sup>53</sup> functional and the Vanderbilt ultrasoft pseudopotentials.<sup>65</sup> An energy cutoff of 25 Ry was used. The initial configuration was relaxed by six short CPMD runs comprising 200 steps. After each run, the system was quenched to the Born–Oppenheimer surface by reoptimizing the wave function. Longer 48 ps production runs were then performed with a temperature of 300 K maintained with the Nosé–Hoover algorithm,<sup>66</sup> which also kept the system in the canonical (NVT) ensemble. During the long simulations, the trajectory was saved at every 50th step. The calculation took about 6.5 weeks using four processors (Intel Xeon 2.4 GHz). Unfortunately, for 2-aminopropanol, the method did not provide a realistic conformer distribution. The simulation time was still too short to enable conformational transitions, such as torsion angle rotations. Thus, only the MD computations were used for this molecule. For lactamide, which has a more limited conformational freedom, the time limitation was partially overcome by performing two independent CPMD simulations, for the starting O–C–N torsion angle of 0° and 180°.

**Extraction of the Clusters and Their Optimization.** From the classical MD trajectories, solute molecules were extracted with varying number of surrounding waters, considering (i) water molecules hydrogen-bonded to the solute and positioned less than 3.6 Å from the solute, resulting in clusters with 5–12 water molecules, (ii) all water molecules closer than 3.6 Å to the

solute, resulting in clusters with 9–16 water molecules (this case approximately corresponds to the complete first water solvation shell), and (iii) all water molecules closer than 5.0 Å to the solute, resulting in clusters containing 23–35 water molecules (corresponding to the first and second water solvation shell). For the smaller CPMD clusters, solute geometries were extracted with the first hydrogen-bonded water shell (3.5 Å, in total 4–9 water molecules) only. Following the extraction, cluster geometries were optimized employing the normal mode optimization procedure<sup>67,68</sup> at the B3LYP/6-311++G(d,p)/CPCM level. The modes within  $i300-300\text{ cm}^{-1}$  were kept fixed, which ensured a minimal change of the MD geometry under the necessary relaxation of the higher frequency modes most important for the spectra. The program QGRAD<sup>69</sup> interfaced to GAUSSIAN<sup>56</sup> was used for the optimization.

**ROA and Raman Spectra Generation.** Harmonic vibrational frequencies, Raman, and Raman optical activity intensities were computed at the B3LYP/6-311++G(d,p)/CPCM level (using gauge-including atomic orbitals, GIAO) with an incident light frequency of 532 nm by GAUSSIAN. Control calculations employing the aug-cc-pVTZ basis set were also performed, resulting in very similar spectra. A discussion of the suitability of the B3LYP method and further tests of basis sets for ROA can be found in earlier works.<sup>14,43,70–72</sup> The spectral shapes were simulated using Lorentzian peaks with a bandwidth of  $10\text{ cm}^{-1}$ , unless otherwise indicated. The Boltzmann temperature correction was considered for the backscattered Raman and ROA intensities.<sup>2,73</sup> The spectral signal originating from water itself was removed from all spectra by setting the polarizability derivatives of water atoms to zero. The intensities were normalized to one cluster (solute molecule). To facilitate the comparison between theory and experiment, the experimental Raman intensity was scaled so that the total integral area between 600 and 1550  $\text{cm}^{-1}$  was the same as calculated. The same scaling factor was used for ROA, so that the circular intensity difference (CID)<sup>1</sup> ratio was unchanged.

## RESULTS AND DISCUSSION

**Lactamide Geometry from QM Calculations.** The conformational space of lactamide was first explored in vacuum and with CPCM, by performing systematic scans of the potential energy surface. The DFT computations in vacuum are not directly relevant to our experiment. However, the geometrical parameters of the stable structures can be compared to an earlier free jet spectroscopic study of Maris et al.<sup>74</sup> The rotational millimeter wave spectrum of lactamide indicated the presence of two conformations, anti and syn with respect to the position of the OH and CO groups. In the same work, calculations showed that for the anti conformation, three stable local minima exist, which differ in the OH orientation. Our method (B3LYP/aug-cc-pVTZ, for both vacuum and the CPCM solvent correction, Table 1 and Figure 2) provides similar results, indicating four stable lactamide conformers with relative enthalpies ( $\Delta H^{298\text{ K}}$ ) below 1.2 kcal/mol.

The conformers I–III belong to the anti family, stabilized by an intramolecular hydrogen bond between NH<sub>2</sub> and OH (of the type (N)H···O(H)), in both vacuum and CPCM. They exhibit similar  $\psi$  torsion angles ( $\angle\text{N,C,C,C}$ ; from  $-107^\circ$  to  $-131^\circ$ ), but the  $\chi_{\text{OH}}$  angle is specific for each conformer. In vacuum, for example, the OH proton adopts three different orientations, in plane with NH<sub>2</sub> (II,  $\chi_{\text{OH}} = -173.6^\circ$ ), out of plane pointing away from CH<sub>3</sub> (I,  $\chi_{\text{OH}} = 82.5^\circ$ ), and out of plane pointing toward CH<sub>3</sub>

**Table 1.** Low-Energy (*R*)-Lactamide Conformers (cf. Figure 2), Calculated (B3LYP) Torsion Angles,<sup>a</sup> Relative Enthalpies ( $\Delta H^{298\text{K}}$ , kcal/mol), and Boltzmann Populations (% in Parentheses)

| conf | vac <sup>b</sup> |                          | CPCM <sup>b</sup> |                          | vac <sup>b</sup>         | CPCM <sup>c</sup>        | IEFPCM <sup>b</sup>      | CPCM <sup>b</sup>        |
|------|------------------|--------------------------|-------------------|--------------------------|--------------------------|--------------------------|--------------------------|--------------------------|
|      | $\psi$ (deg)     | $\chi_{\text{OH}}$ (deg) | $\psi$ (deg)      | $\chi_{\text{OH}}$ (deg) | $\Delta H^{298\text{K}}$ | $\Delta H^{298\text{K}}$ | $\Delta H^{298\text{K}}$ | $\Delta H^{298\text{K}}$ |
| I    | -106.7           | 82.5                     | -107.5            | 77.6                     | 0.00 (14)                | 0.00 (55)                | 0.00 (57)                | 0.00 (57)                |
| II   | -119.0           | -173.6                   | -122.1            | 158.9                    | -0.40 (28)               | 0.38 (29)                | 0.49 (25)                | 0.48 (25)                |
| III  | -129.8           | -98.3                    | -130.5            | -79.0                    | -0.01 (14)               | 1.12 (8)                 | 1.09 (9)                 | 1.07 (9)                 |
| IV   | 64.5             | -4.1                     | 89.5              | -51.2                    | -0.67 (44)               | 1.22 (7)                 | 1.13 (9)                 | 1.12 (9)                 |

<sup>a</sup> For definition of angles see Figure 2. <sup>b</sup> The aug-cc-pVTZ basis. <sup>c</sup> 6-311++G(d,p) basis.

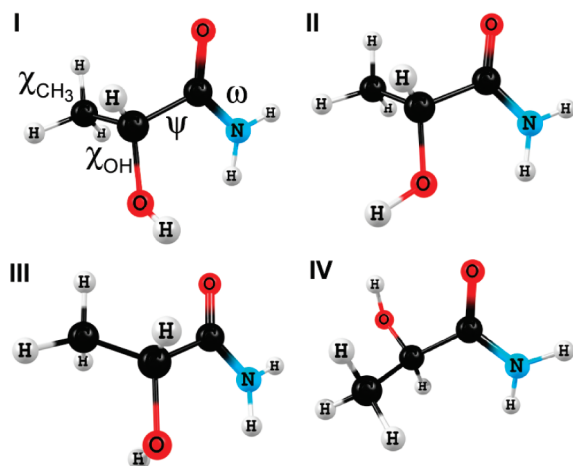


**Figure 2.** Four lowest energy (B3LYP/aug-cc-pVTZ/CPCM) conformers of (*R*)-lactamide and the characteristic angles ( $\omega = \angle(\text{H}, \text{N}, \text{C}, \text{C})$ , the hydrogen was chosen for  $\omega$  to be close to  $0^\circ$ ;  $\psi = \angle(\text{N}, \text{C}, \text{C}, \text{C})$ ;  $\chi_{\text{CH}_3} = \angle(\text{C}, \text{C}, \text{C}, \text{H})$ ,  $\chi_{\text{OH}} = \angle(\text{C}(\text{O}), \text{C}, \text{O}, \text{H})$ ).

(III,  $\chi_{\text{OH}} = -98.3^\circ$ ). Conformer IV exhibits a syn conformation ( $\psi = 64.5^\circ$  in vacuum and  $89.5^\circ$  in CPCM) and an internal (O)H $\cdots$ O(=C) hydrogen bond.

Although the geometries of the vacuum and CPCM structures can be clearly related to each other, the solvent has a significant influence on their stability. According to the calculations (Table 1), conformer IV is energetically favored in vacuum (44% of the Boltzmann population, in excellent agreement with the free jet experiment predicting a  $\sim 50\%$  ratio<sup>74</sup>), but it becomes the least favored form in CPCM (9%). The dominant CPCM conformation (conformer I, 57% of the Boltzmann population) is disfavored in vacuum (9% of the Boltzmann population, Table 1). The CPCM geometries are more relevant than the vacuum structures for the present work, as they should be closer to the experimental lactamide conformations found in aqueous solutions.

Employing a different basis set (6-311++G(d,p)) or a different PCM model (IEFPCM) has very little influence on the energetic distribution of conformers (Table 1; for electronic and Gibbs free energies and for MP2 results see Tables S1 and S2 in the Supporting Information). Thus, we will assume that the calculated distribution of the conformers is reliable enough to be used for approximate averaging of the spectra.

**Lactamide Geometry from MD and CPMD Calculations.** An analysis of the lactamide conformers generated with dynamical (MD and CPMD) methods shows qualitative agreement with the PCM equilibrium structures (Figure 3). However, the dynamics provides a broad angular distribution of the angles  $\psi$

and  $\chi_{\text{OH}}$ . For  $\psi$ , the MD probability (black line in Figure 3) has a maximum around  $70^\circ$ , which approximately corresponds to the syn conformer IV. The CPMD probability curve (obtained as an average of the two CPMD runs) is presumably more accurate, centered around  $-120^\circ$ , which corresponds to the anti conformers I–III, preferred also by CPCM. As indicated in the Methodology section, the CPMD dynamics simulation was too short to ensure sufficient sampling for the  $\psi$ -rotation (see also the time dependence of the MD and CPMD angles in Figure S1 of the Supporting Information), and an accurate  $\psi$ -angle distribution cannot be obtained from this method in a reasonable computational time. By comparing the potential of mean force in vacuum and water for the  $\psi$ -rotation (Figure S2), it can be clearly seen that water largely expands the range populated by this angle; thus, the molecule becomes more flexible when hydrated. However, we consider the CPCM conformer energies and distributions to be more accurate than those obtained from the empirical Amber99 force field, which apparently overestimates the syn-type conformers.

The  $\chi_{\text{OH}}$  MD distribution, also plotted in Figure 3, corresponds well to the CPCM results for conformers I–III (Table 1). The CPMD runs provide a qualitatively different curve, centered around  $110^\circ$ , indicating a preference for solute–solvent hydrogen bonding. The absence of the opposite  $\chi_{\text{OH}}$  angle of  $-110^\circ$  in the CPMD distribution suggests a strong influence of the asymmetric carbon atom, perhaps strengthened by the water hydrogen bond network as discussed previously for alanine.<sup>75</sup> The strong hydration is also reflected in the radial distribution functions (Figure S3 in Supporting Information). These distributions, however, may be somewhat affected by the limited simulation time of the CPMD simulation. The MD and CPMD distributions of the  $\omega$  and  $\chi_{\text{CH}_3}$  angles are nearly identical (Figure 3).

**Spectra of Lactamide and Normal Mode Assignment at the PCM Level of Theory.** The Raman and ROA spectra for the lactamide conformers obtained at the CPCM level of theory (B3LYP/6-311++G(p,d)/CPCM) are compared to the experimental spectra in Figure 4. The calculated spectra for the individual CPCM conformers I–IV show a strong conformational dependence (Figure S4, Supporting Information). The averaged spectra (Figure 4) are based on the Boltzmann distribution of the four CPCM conformers I–IV (Table 1).

The Raman spectra simulated by means of CPCM show reasonable agreement with experiment, so we used these for the assignment of the experimental Raman peaks. On the basis of this, we have assigned the peaks, for example to the  $\text{NH}_2$  wagging ( $812\text{ cm}^{-1}$ ), in-phase C–C–O stretching ( $920\text{ cm}^{-1}$ ), out-of-phase C–C–O stretching ( $1047\text{ cm}^{-1}$ ), C–C stretching ( $1089\text{ cm}^{-1}$ ), C=O stretching ( $1586\text{ cm}^{-1}$ ), and  $\text{NH}_2$  bending ( $1675\text{ cm}^{-1}$ ). The assignment is problematic in the 1200–1500

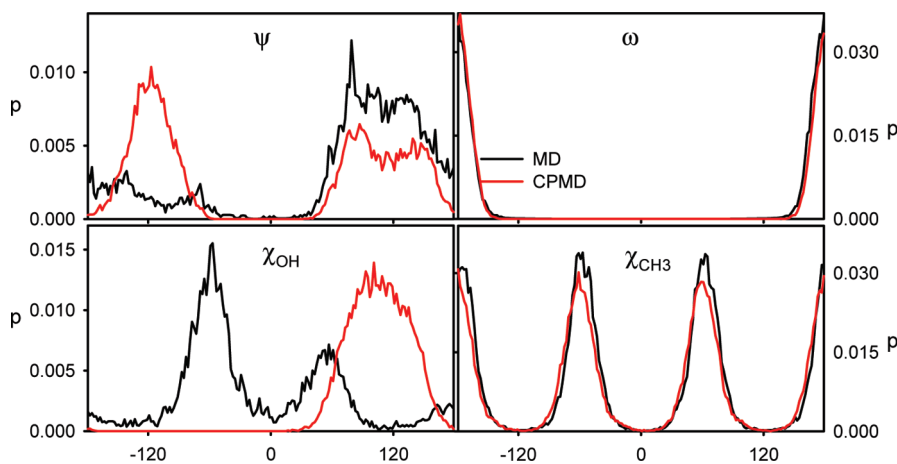


**Figure 3.** (*R*)-Lactamide angular distributions obtained by the classical MD (Amber99 FF, 1 ns run) and CPMD (two averaged 48 ps runs, for definition of angles see Figure 2).

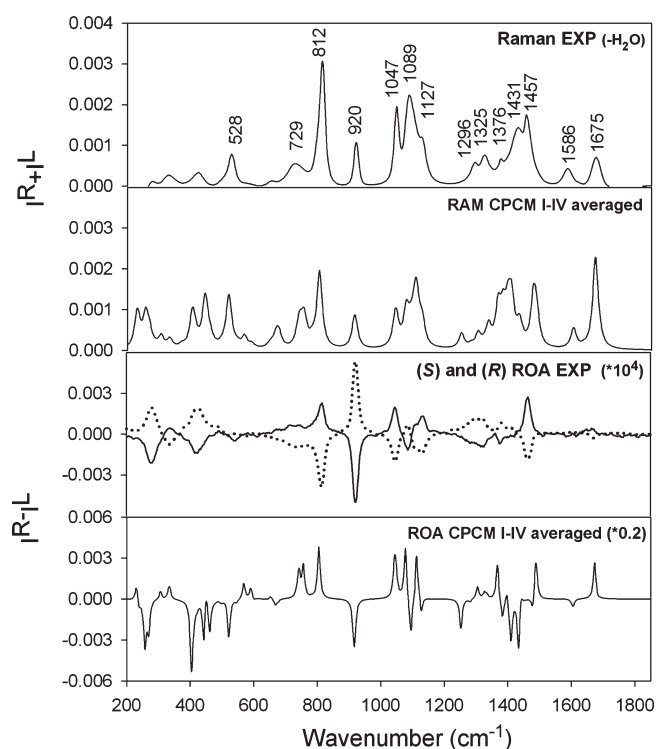


**Figure 4.** Experimental (first and third panels) and computed (second and fourth panels) Raman and ROA spectra of (*R*)-lactamide (solid line) and (*S*)-lactamide (dotted line). Computations were done at the B3LYP/6-311++G(d,p)/CPCM level; conformers I–V were averaged using the weights in Table 1.

wavenumber region because there in this region is a high density of CH bending modes and because the calculated and experimental spectra match only approximately. The experimental intensities around  $1650\text{ cm}^{-1}$  can be affected by an incomplete subtraction of the water (HOH bending) signal.

In the experimental ROA spectra of lactamide, the (*R*)- and (*S*)-enantiomers provide opposite signals, as expected (Figure 4, third panel). We note, however, that especially the part around  $812\text{ cm}^{-1}$  was difficult to measure due to occasional artifacts coming from the strongly polarized Raman band and background

fluorescence of impurities. The influence of the impurities could be significantly quenched by purification and by leaving the sample for several hours in the laser beam. Unlike for Raman, the computed and experimental ROA spectra for (*R*)-lactamide show only moderate agreement (Figure 4, third and fourth panels). Most peaks are reproduced with correct signs; however, even the Boltzmann-averaged CPCM spectrum contains many sharp peaks that are not observed experimentally.

**Spectral Improvement by *Ad Hoc* Explicit Hydration.** The importance of explicit hydration is documented by simple QM cluster models, where water molecules are manually added to all polar groups of the CPCM equilibrium structures of lactamide (Figure 5; the Raman and ROA spectra of individual clusters can be seen in Figures S5 of Supporting Information). The ROA spectra of the hydrated clusters are then computed in combination with CPCM (in order to model the long-range electrostatic effects of the surrounding bulk water). For the hydrated clusters, we estimated the Boltzmann weights for the averaging based on single-point enthalpies of the solute structures only, which resulted in weights somewhat different from those in Table 1 (22, 41, 35, and 2% for 4W–I, 4WII, 4W–III, and 4W–IV, respectively). The averaged ROA spectrum (Figure 5) shows several significantly improved features compared to the plain CPCM structures (Figure 4). The region from  $800\text{ to }1200\text{ cm}^{-1}$  is now fairly well reproduced, with no excess peaks in the computed spectra. Here, the explicit hydrogen bonding caused a frequency shift, grouping different individual peaks together. Using a different number of water molecules (e.g., three or five) or a different hydrogen-bonding pattern, however, leads to different spectra (see for instance the ROA spectrum with three explicit water molecules in Figure S6 of the Supporting Information). An additional practical drawback of the *ad hoc* approach is the notoriously slow convergence of a complete geometry optimization of the clusters<sup>68</sup> due to the shallow nature of the potential energy surface.

**Spectral Simulations with MD Snapshots.** A more automated and more rigorous approach for generation of hydrated lactamide conformations is through the use of dynamical methods such as classical MD or CPMD. The Raman and ROA spectra for lactamide obtained from 1000 hydrated MD clusters (with 5–12 water molecules) extracted from snapshots corresponding to 10 ns of MD simulation are shown in Figure S7.

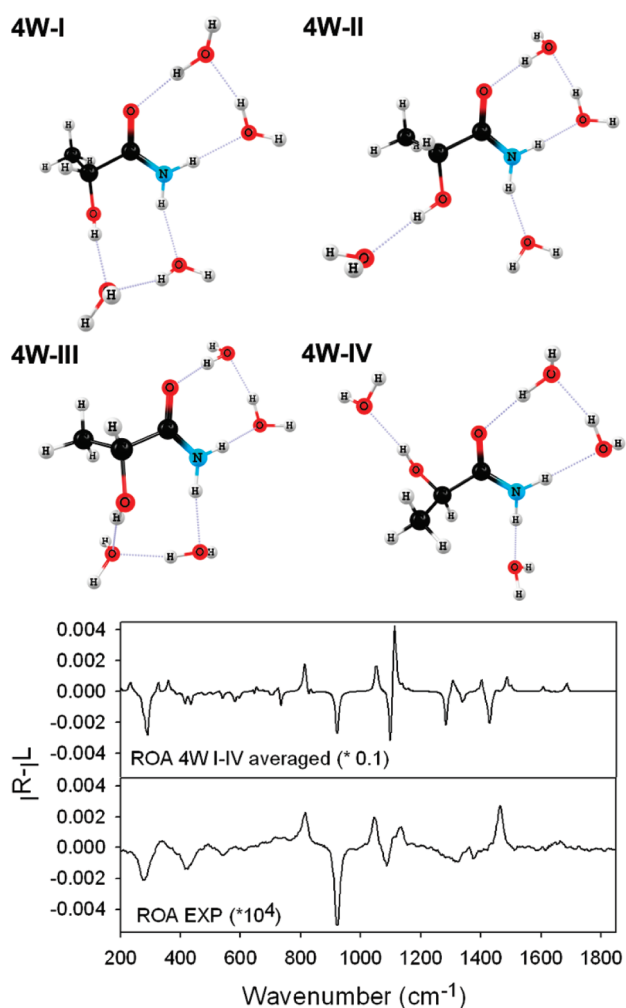


**Figure 5.** Computed averaged ROA spectrum and comparison to experimental spectrum (bottom) of hydrated lactamide clusters with four explicit water molecules (4W-I to 4W-IV, top).

Raman and ROA spectra obtained on the basis of 2000 hydrated CPMD clusters (4–9 water molecules) extracted from snapshots corresponding to two CPMD runs of each 48 ps are shown in Figure S8. In all spectra calculations, the effect of the surrounding bulk water was treated with the CPCM model.

The generated ROA spectra for lactamide and for the second model compound, 2-aminopropanol, are compared to all employed solvation models (CPCM, 4W, MD, CPMD) in Figure 6 (for optimized conformers of 2-aminopropanol see Figure S9). A comparison of the corresponding Raman spectra for all simulations is shown in Figure S10.

The third spectrum from the top in Figure 6 was obtained from molecular dynamics snapshots. One can observe that this procedure leads to better agreement of the calculated ROA spectrum with experiment than either plain CPCM (first panel) or *ad hoc* explicit hydration (second panel), although the peak pattern in the region between 1000 and 1200  $\text{cm}^{-1}$  is better reproduced by *ad hoc* explicit hydration. The Raman spectrum (Figure S10 in Supporting Information), however, is in better agreement with experiment when MD is employed. The MD averaging improves even the Raman profile of the CH bending region at 1300–1500  $\text{cm}^{-1}$  (Figure S10), although we believe that errors in the exchange-correlation functional and

anharmonic interactions<sup>76</sup> limit the accuracy more. The advantages of MD are also visible in the ROA spectra of 2-aminopropanol, particularly in the region from 200 to 1000  $\text{cm}^{-1}$ , which is almost the same in the experimental and MD spectra, while the use of *ad hoc* explicit hydration produces some features not found in the experimental spectrum.

In spite of the higher CPU time (Figure 6, left), the MD cluster averaging thus represents a more elegant and straightforward method to generate the spectra of explicitly hydrated systems, provided that automatic computer scripts for the cluster manipulation are available. We also found that normal mode partial optimization of the clusters was an essential part of the simulations; indeed, quite unreasonable spectral curves were produced with raw MD clusters (see for example Figure S11 of the Supporting Information). The optimization is necessary in order to relax the high-frequency modes contributing the most to the spectra, leading to much better spectral profiles.

**Car–Parrinello versus Conventional MD.** CPMD simulations lead, in the case of lactamide, to a ROA spectrum in better agreement with experiment than classical MD (compare spectra in third and fourth rows of Figure 6), even though the CPMD time frame (48 ps) was, by necessity, much shorter. Because of the time limits, the CPCM ratios were used to mix the spectra generated by separate runs for the syn and anti conformations (9 and 91%, respectively, based on the CPCM distribution of syn and anti conformers; for individual ROA and Raman spectra see Figure S8 of the Supporting Information). Classical MD seems to overestimate the inhomogeneous band broadening, which results in a too low ROA signal, while the CPMD bandwidths and relative intensities are more realistic. Nevertheless, it should be noted that also the CPMD curves deviate from experiment, which can be attributed to the complex structure and dynamics of the hydrated molecules and to the approximations used in the calculations (such as the chosen functional, harmonic limit, and the semiquantum approach to the vibrational motions). As pointed out above, for 2-aminopropanol it was not possible to obtain a sufficient number of uncorrelated CPMD snapshots in a reasonable time frame (the simulation time was too short to allow the system to move between different conformational basins), and the CPMD results are therefore not shown in this case. We therefore note that CPMD, although in principle the most rigorous method of accounting for hydration effects, may not be practical in the case of larger conformationally flexible systems, and MD or even *ad hoc* explicit hydration methods may be more useful.

**First and Second Water Shell Contributions.** In order to gain additional insight into the influence of the surrounding water shells, we extracted three types of hydrated lactamide clusters from the MD snapshots: (i) clusters with hydrogen-bonded water molecules within a distance of 3.6 Å from the solute, which essentially corresponds to the first hydrogen-bonded hydration shell (in total 5–12 waters per cluster), (ii) clusters with all water molecules within a distance of 3.6 Å from the solute, corresponding to the first complete water shell (9–16 water molecules), and (iii) clusters with all water molecules within a distance of 5.0 Å from the solute, corresponding to the complete first and second water shell (with 23–35 water molecules per cluster). Following the normal mode optimizations, the ROA spectra were computed for 100 clusters (corresponding to 1 ns of MD simulation, Figure 7). In the ROA calculations, CPCM was employed to treat effects from the surrounding bulk water.

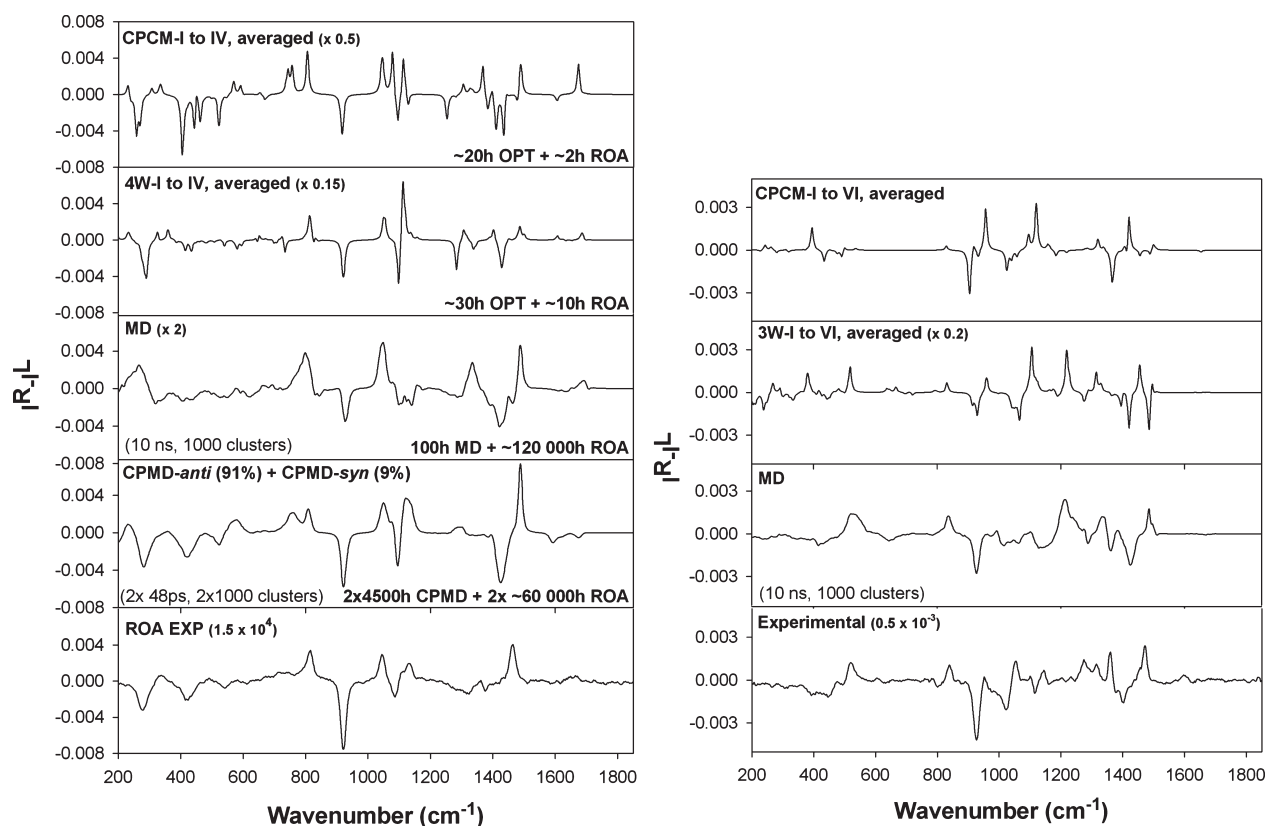


**Figure 6.** Comparison of ROA spectra of (*R*)-lactamide (left) and (*S*)-2-aminopropanol (right) computed by the different hydration models and experiment. Approximate computational times for calculations are indicated for each method (left, the shown values correspond to the total on all conformers/clusters, OPT = full QM optimization, for the MD and CPMD clusters ROA = normal mode optimization + ROA calculation).

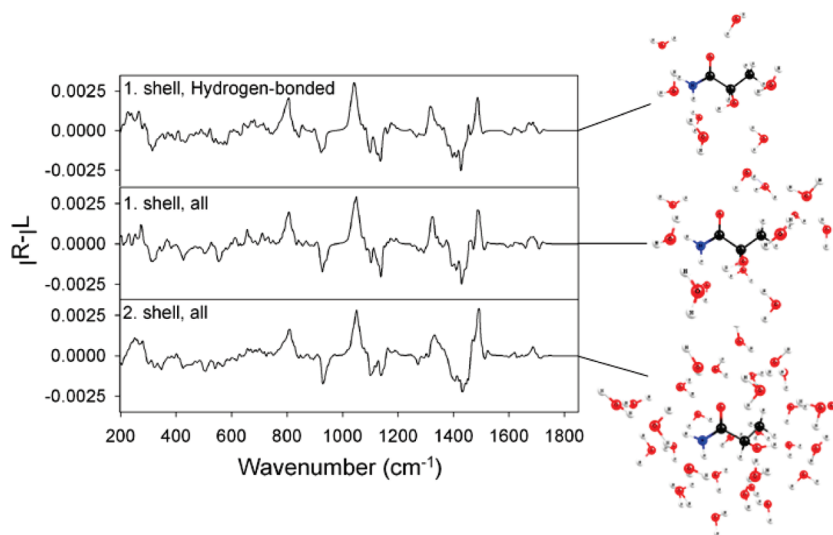


**Figure 7.** Effect of water shells on computed ROA spectrum of lactamide (average over 100 MD clusters corresponding to 1 ns simulation): clusters (top) with hydrogen-bonded waters within 3.6 Å, (middle) with all waters closer than 3.6 Å, and (bottom) all waters within 5 Å.

The generated ROA spectra for the three cluster types are very similar, indicating that already the first hydrogen-bonded water shell reproduces most of the effect of water on the spectral properties of lactamide. Thus, the water molecules bound most strongly to the solute have the largest effect on the ROA spectra, as was also observed in the case of NMR properties.<sup>38</sup>

**Dependence on the Number of Clusters.** A very important practical aspect concerns the convergence, that is, the number of MD snapshots that need to be included in the generation of realistic Raman and ROA spectra. We have here generated spectra based on 10–1000 MD snapshots, each spanning 1 ns of simulation time (see Figures S12 and S13 for the spectra and

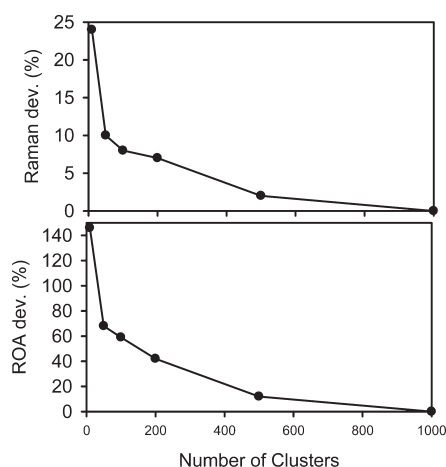


**Figure 8.** Convergence of the Raman and ROA lactamide spectral errors with respect to the number of averaged MD snapshots, relative to the normalized spectra obtained from 1000 snapshots ( $\text{dev} \sim \int |S - S_{1000}| d\omega$ ).

their differences). By taking the difference between the spectrum with the largest number of snapshots (1000) and the spectra with fewer snapshots, it is possible to approximately evaluate the error of the limited number of snapshots, as in Figure 8. The convergence is relatively slow; the error approximately decays as  $1/\sqrt{N}$ . Significantly more clusters are needed to achieve a good accuracy of the ROA spectrum than for the Raman spectrum. As an additional test, we simulated Raman and ROA spectra of glycine (which is achiral), providing similar results (Figure S14 of Supporting Information) and also indicating that the ROA/Raman error ratio converges as  $\sim 1/\sqrt{N}$ . Our calculations showed that the ROA spectrum simulated for glycine is reduced to zero only when more than 500 snapshots are used, while the appearance of the Raman spectrum changes little between 100 and 500 snapshots. Given that a typical experimental accuracy of the intensities is about 10%, 50 and 500 clusters are needed for a reliable simulation of the Raman and ROA intensities, respectively. However, as suggested by the *ad hoc* model presented above, and by the MD simulations (Figures S12 and S13, Supporting Information), a much smaller number of averaged structures can already produce the main trends caused by the hydration.

## CONCLUSIONS

We have investigated the role of the aqueous environment on the Raman and Raman optical activity (ROA) spectra of two conformationally flexible and strongly hydrated compounds: lactamide and 2-aminopropanol. The hydration models included polarizable continuum models, explicit *ad hoc* hydration, and two dynamical approaches, classical MD and CPMD. We have found that the PCM approaches gave basic information about molecular conformational energies, vibrational normal modes, and Raman and ROA intensity patterns. However, the presence of explicit water molecules was required to provide better agreement with experimental spectra, including the inhomogeneous broadening of spectral bands, and finer intensity changes caused by the solvation. The results clearly show that cluster averaging is the most universal method, with which most of the spectral features can be explained. Nonetheless, because of intrinsic errors of all the approaches used to model the solvated compounds, simpler models may suffice for many practical simulations. The CPCM model with conformational averaging

provided reasonable Raman profiles, explaining most of the experimental observations. Qualitatively correct ROA spectra, however, required inclusion of explicit waters, at least in the *ad hoc* static model. The spectral profiles could be further improved by the dynamical averaging. In this respect, the CPMD results are superior to MD, provided that the simulation time is long enough to allow for accessing of the entire conformational space.

Although superior to CPCM and vacuum calculations, the dynamical runs display some shortcomings. The quantum character of the vibrations requires using the empirical normal mode optimization scheme<sup>67,68</sup> to correct the raw MD geometries. The MD (Amber) force field appears to generate somewhat unrealistic conformer ratios, while CPMD suffers from an extensive computer cost (months of CPU time). For 2-aminopropanol, CPMD did not provide useful conformer distributions at all. The computed ROA spectra show slow convergence with respect to the number of included clusters, implying that averaging should be done over a relatively large number of snapshots. Finally, some inaccuracies in the spectra, especially in the CH bending region, may be caused by anharmonic interactions and errors of the DFT method, but a detailed analysis of these sources of errors goes beyond the scope of this study.

Despite these shortcomings, we can conclude that the multi-scale approach employed here (combining molecular dynamics, quantum mechanics, and normal mode optimization) in combination with feasible ROA calculations (enabled by fast analytical DFT calculations of the optical activity tensors) does allow for the generation of realistic spectra for the model compounds lactamide and 2-aminopropanol. The approach presented is able to reveal interesting details about the structure, dynamics, and interactions with the environment and thus provides a feasible basis for the generation of ROA spectra of biologically interesting molecules.

## ASSOCIATED CONTENT

**S Supporting Information.** Computed relative energies for lactamide conformers employing different methods (Tables S1 and S2) and additional details of the computational results (Figures S1–S14). This material is available free of charge via the Internet at <http://pubs.acs.org>.

## AUTHOR INFORMATION

### Corresponding Author

\*E-mail [kathrin.hopmann@uit.no](mailto:kathrin.hopmann@uit.no), Tel +47 776 23109, Fax +47 776 44765 (K.H.H.); e-mail [bour@uochb.cas.cz](mailto:bour@uochb.cas.cz), Tel (+420)220183348, Fax (+420)220183578 (P.B.).

## ACKNOWLEDGMENT

The work was supported by the Grant Agency of the Academy of Sciences (M200550902), KONTAKT II MSMT program (LH11033), Grant Agency of the Czech Republic (P208/11/0105), Norwegian Research Council through a Center of Excellence Grant (No. 179568/V30) and Research Grant No. 191251/V00, by a grant of computer time from the Norwegian Supercomputing Program (Notur), and by the Ministry of Science and Higher Education (Poland) from funds for scientific research in years 2009–2011 as Project No. N N204 138637.

## REFERENCES

- (1) Barron, L. D. *Molecular Light Scattering and Optical Activity*; Cambridge University Press: Cambridge, 2004.
- (2) Polavarapu, P. L. *Vib. Spectra Struct.* **1984**, *13*, 103.
- (3) Polavarapu, P. L. *Angew. Chem., Int. Ed.* **2002**, *41*, 4544.
- (4) Kapitán, J.; Baumruk, V.; Kopecký, V., Jr.; Bouř, P. *J. Phys. Chem. A* **2006**, *110*, 4689.
- (5) Zhu, F.; Isaacs, N. W.; Hecht, L.; Barron, L. D. *J. Am. Chem. Soc.* **2005**, *127*, 6142.
- (6) Kapitán, J.; Baumruk, V.; Kopecký, V., Jr.; Bouř, P. *J. Am. Chem. Soc.* **2006**, *128*, 2438.
- (7) McColl, I. H.; Blanch, E. W.; Hecht, L.; Kallenbach, N. R.; Barron, L. D. *J. Am. Chem. Soc.* **2004**, *126*, 5076.
- (8) Barron, L. D.; Blanch, E. W.; Hecht, L. *Adv. Protein Chem.* **2002**, *62*, 51.
- (9) Syme, C. D.; Blanch, E. W.; Holt, C.; Jakes, R.; Goedert, M.; Hecht, L.; Barron, L. D. *Eur. J. Biochem.* **2002**, *269*, 148.
- (10) Barron, L. D.; Hecht, L.; Blanch, E. W.; Bell, A. F. *Prog. Biophys. Mol. Biol.* **2000**, *73*, 1.
- (11) Blanch, E. W.; McColl, I. H.; Hecht, L.; Nielsen, K.; Barron, L. D. *Vib. Spectrosc.* **2004**, *35*, 87.
- (12) Abdali, S. J. *Raman Spectrosc.* **2006**, *37*, 1341.
- (13) Osinska, K.; Pecul, M.; Kudelski, A. *Chem. Phys. Lett.* **2010**, *496*, 86.
- (14) Ruud, K.; Helgaker, T.; Bouř, P. *J. Phys. Chem. A* **2002**, *106*, 7448.
- (15) Haesler, J.; Schindelholz, I.; Riguet, E.; Bochet, C. G.; Hug, W. *Nature* **2007**, *446*, 526.
- (16) Buděšínský, M.; Daněček, P.; Bednářová, L.; Kapitán, J.; Baumruk, V.; Bouř, P. *J. Phys. Chem. A* **2008**, *112*, 8633.
- (17) Jalkanen, K. J.; Nieminen, R. M.; Knapp-Mohammady, M.; Suhai, S. *Int. J. Quantum Chem.* **2003**, *92*, 239.
- (18) Tajkhorshid, E.; Jalkanen, K. J.; Suhai, S. *J. Phys. Chem. B* **1998**, *102*, 5899.
- (19) Bouř, P.; Michalík, D.; Kapitán, J. *J. Chem. Phys.* **2005**, *122*, 144501.
- (20) Kapitán, J.; Baumruk, V.; Kopecký, V., Jr.; Pohl, R.; Bouř, P. *J. Am. Chem. Soc.* **2006**, *128*, 13451.
- (21) Onsager, L. *J. Am. Chem. Soc.* **1936**, *58*, 1486.
- (22) Wong, M. W.; Frisch, M. J.; Wiberg, K. B. *J. Am. Chem. Soc.* **1991**, *113*, 4776.
- (23) Klamt, A.; Schuurmann, G. *J. Chem. Soc., Perkin Trans.* **1993**, *2*, 799.
- (24) Tomasi, J.; Mennucci, B.; Cammi, R. *Chem. Rev.* **2005**, *105*, 2999.
- (25) Cancès, E.; Mennucci, B.; Tomasi, J. *J. Chem. Phys.* **1997**, *107*, 3032.
- (26) Barone, V.; Cossi, M. *J. Phys. Chem. A* **1998**, *102*, 1995.
- (27) Cossi, M.; Rega, N.; Scalmani, G.; Barone, V. *J. Comput. Chem.* **2002**, *24*, 669.
- (28) Cossi, M.; Barone, V. *J. Chem. Phys.* **1998**, *109*, 6246.
- (29) Bouř, P. *J. Chem. Phys.* **2004**, *121*, 7545.
- (30) Mennucci, B.; Martínez, J. M. *J. Phys. Chem. B* **2005**, *109*, 9818.
- (31) Cappelli, C.; Corni, S.; Mennucci, B.; Cammi, R.; Tomasi, J. *J. Phys. Chem. A* **2002**, *106*, 12331.
- (32) Jalkanen, K. J.; Degtyarenko, I. M.; Nieminen, R. M.; Cao, X.; Nafie, L. A. *Theor. Chem. Acc.* **2008**, *119*, 191.
- (33) Šebek, J.; Kejlik, Z.; Bouř, P. *J. Phys. Chem. A* **2006**, *110*, 4702.
- (34) Caricato, M.; Ingrosso, F.; Mennucci, B.; Tomasi, J. *J. Chem. Phys.* **2005**, *122*, 154501.
- (35) Caricato, M.; Mennucci, B.; Tomasi, J.; Ingrosso, F.; Cammi, R.; Corni, S.; Scalmani, G. *J. Chem. Phys.* **2006**, *124*, 124520.
- (36) Mikkelsen, K. V.; Ruud, K.; Helgaker, T. *Chem. Phys. Lett.* **1996**, *253*, 443.
- (37) Kongsted, J.; Ruud, K. *Chem. Phys. Lett.* **2008**, *451*, 226.
- (38) Dračinský, M.; Bouř, P. *J. Chem. Theory Comput.* **2010**, *6*, 288.
- (39) Corni, S.; Cappelli, C.; Cammi, R.; Tomasi, J. *J. Phys. Chem. A* **2001**, *105*, 8310.
- (40) Pecul, M.; Lamparska, E.; Cappelli, C.; Frediani, L.; Ruud, K. *J. Phys. Chem. A* **2006**, *100*, 2807.
- (41) Pecul, M. *Chirality* **2009**, *21*, E98.
- (42) Bondesson, L.; Mikkelsen, K. V.; Luo, Y.; Garberg, P.; Ågren, H. *Spectrochim. Acta, Part A* **2007**, *66*, 213.
- (43) Šebek, J.; Kapitán, J.; Šebestík, J.; Baumruk, V.; Bouř, P. *J. Phys. Chem. A* **2009**, *113*, 7760.
- (44) Mukhopadhyay, P.; Zuber, G.; Beratan, D. N. *Biophys. J.* **2008**, *95*, 5574.
- (45) Ruud, K.; Thorvaldsen, A. J. *Chirality* **2009**, *21*, E54.
- (46) Cheeseman, J. R. Calculation of Molecular Chiroptical Properties Using Density Functional Theory; CD 2007, Groningen, 2007.
- (47) Liegeois, V.; Ruud, K.; Champagne, B. *J. Chem. Phys.* **2007**, *127*, 204105.
- (48) Dračinský, M.; Kaminský, J.; Bouř, P. *J. Phys. Chem. B* **2009**, *14698*.
- (49) Car, R.; Parrinello, M. *Phys. Rev. Lett.* **1985**, *55*.
- (50) Hug, W.; Hangartner, G. *J. Raman Spectrosc.* **1999**, *30*, 841.
- (51) Hug, W. *Appl. Spectrosc.* **2003**, *57*, 1.
- (52) Zhu, F. J.; Isaacs, N. W.; Hecht, L.; Barron, L. D. *Structure* **2005**, *13*, 1409.
- (53) Becke, A. D. *J. Chem. Phys.* **1993**, *98*, 5648.
- (54) Lee, C.; Yang, W.; Parr, R. G. *Phys. Rev. B* **1988**, *37*, 785.
- (55) Dunning, T. H.; Peterson, K. A.; Woon, D. E. Basis sets: Correlation consistent basis sets. In *Encyclopedia of Computational Chemistry*; Schleyer, P. R., Allinger, N. L., Clark, T., Gasteiger, J., Kollman, P. A., Schaefer III, H. F., Schreiner, P. R., Eds.; Wiley: Chichester, 1998; Vol. 1, p 88.
- (56) Frisch, M. J.; Trucks, G. W.; Schlegel, H. B.; Scuseria, G. E.; Robb, M. A.; Cheeseman, J. R.; Scalmani, G.; Barone, V.; Mennucci, B.; Petersson, G. A.; Nakatsuji, H.; Caricato, M.; Li, X.; Hratchian, H. P.; Izmaylov, A. F.; Bloino, J.; Zheng, G.; Sonnenberg, J. L.; Hada, M.; Ehara, M.; Toyota, K.; Fukuda, R.; Hasegawa, J.; Ishida, M.; Nakajima, T.; Honda, Y.; Kitao, O.; Nakai, H.; Vreven, T.; Montgomery, J., Jr.; Peralta, J. E.; Ogliaro, F.; Bearpark, M.; Heyd, J. J.; Brothers, E.; Kudin, K. N.; Staroverov, V. N.; Kobayashi, R.; Normand, J.; Raghavachari, K.; Rendell, A.; Burant, J. C.; Iyengar, S. S.; Tomasi, J.; Cossi, M.; Rega, N.; Millam, J. M.; Klene, M.; Knox, J. E.; Cross, J. B.; Bakken, V.; Adamo, C.; Jaramillo, J.; Gomperts, R.; Stratmann, R. E.; Yazyev, O.; Austin, A. J.; Cammi, R.; Pomelli, C.; Ochterski, J. W.; Martin, R. L.; Morokuma, K.; Zakrzewski, V. G.; Voth, G. A.; Salvador, P.; Dannenberg, J. J.; Dapprich, S.; Daniels, A. D.; Farkas, O.; Foresman, J. B.; Ortiz, J. V.; Cioslowski, J.; Fox, D. J. *Gaussian 09, Revision A.02*; Gaussian, Inc.: Wallingford, CT, 2009.
- (57) Ponder, J. W. *Tinker, Software Tools for Molecular Design*, 3.8 ed.; Washington University School of Medicine: St. Louis, MO, 2000.
- (58) Wang, J.; Cieplak, P.; Kollman, P. A. *J. Comput. Chem.* **2000**, *21*, 1049.
- (59) Rizzo, R. C.; Jorgensen, W. L. *J. Am. Chem. Soc.* **1999**, *121*, 4827.
- (60) Kumar, S.; Bouzida, D.; Swendsen, R. H.; Kollman, P. A.; Rosenberg, J. M. *J. Comput. Chem.* **1992**, *13*, 1011.
- (61) Roux, B. *Comput. Phys. Commun.* **1995**, *91*, 275.
- (62) HyperChem 8.0.3, Hypercube, Inc., Gainesville, 2007.
- (63) Jorgensen, W. L.; Chandrasekhar, J.; Madura, J. D. *J. Chem. Phys.* **1983**, *79*, 926.
- (64) CPMD Version 3.11, IBM Corp., MPI für Festkörperforschung Stuttgart, 2006 (<http://www.cpmid.org>).
- (65) Vanderbilt, D. *Phys. Rev. B* **1990**, *41*, 7892.
- (66) Hoover, W. G. *Phys. Rev. A* **1985**, *31*, 1695.
- (67) Bouř, P.; Keiderling, T. A. *J. Chem. Phys.* **2002**, *117*, 4126.
- (68) Bouř, P. *Collect. Czech. Chem. Commun.* **2005**, *70*, 1315.
- (69) Bouř, P. *Qgrad*; Academy of Sciences: Prague, 2006.
- (70) Reiher, M.; Liegeois, V.; Ruud, K. *J. Phys. Chem. A* **2005**, *109*, 7567.
- (71) Pecul, M.; Ruud, K. *Int. J. Quantum Chem.* **2005**, *104*, 816.
- (72) Pecul, M.; Rizzo, A. *Mol. Phys.* **2003**, *101*, 2073.
- (73) Yamamoto, S.; Straka, M.; Watarai, H.; Bouř, P. *Phys. Chem. Chem. Phys.* **2010**, *12*, 11021.

- (74) Maris, A.; Melandri, S.; Caminati, W.; Favero, P. G. *Chem. Phys.* **2002**, *283*, 111.
- (75) Kaminský, J.; Šebek, J.; Bouř, P. *J. Comput. Chem.* **2009**, *30*, 983.
- (76) Daněček, P.; Kapitán, J.; Baumruk, V.; Bednárová, L.; Kopecký, V., Jr.; Bouř, P. *J. Chem. Phys.* **2007**, *126*, 224513.